Materials Advances

ROYAL SOCIETY OF CHEMISTRY

COMMUNICATION

View Article Online
View Journal | View Issue

Cite this: *Mater. Adv.*, 2023, 4, 5530

Received 22nd September 2023,
Accepted 17th October 2023

DOI: 10.1039/d3ma00747b

rsc.li/materials-advances

Direct evidence of mesogenic dendrons with free void space by Brunauer–Emmett–Teller (BET) isotherms†

Yao-Chih Lu, Jun-Cheng Wang, Yun-He Yang and Long-Li Lai *

Two dendrons with strong dipoles in the central corner were prepared in reasonable yields. Because of the dipole interaction present, the two dendrons were observed to self-assemble into dendrimer-like molecules, which then exhibited mesogenic phases upon thermal treatment. Due to the variation in the length of the central cores, the free pores that are fabricated by two dendrons are different to each other. From the Brunauer–Emmett–Teller (BET) isotherms, the free void space between two dendrons with the shorter central core was observed to be smaller than that for the dendron with a longer central core.

Dendrimers with peripheral groups, connecting units and central cores, may have two- or three-dimensional morphology.[1,2] Due to their characteristics of mono-dispersity and controllable functionalities incorporated at the peripheral, connecting or central moiety during the synthesis, related studies of their specific properties have thus been extensively explored.[3–7] For example, the presence of long alkyl groups at the peripheral part of the dendrimers result in their exhibition of a mesogenic phase upon thermal treatment,[8–12] which further leads the dendritic molecules to self-assemble over a long range, and thus, they have potential as solvating candidates for opto-electronic devices.[13–17] Dendrons with peripheral and connecting moieties are also similar to dendrimers in structure, but only have half the skeleton of dendrimers. The ability of dendrons containing functionalities at the central corner to self-assemble into giant or macromolecules has been extensively reviewed.[18–21] Accordingly, dendrons with NH or OH groups at the central corner and long alkyl groups at their periphery may also assemble into dendrimer-like molecules and then exhibit mesogenic properties upon thermal treatment, although the reported examples are rather limited in comparison with examples of mesogenic dendrimers.[22–33] Possibly, dendrimers with symmetrical structures are more favorable for the formation of liquid crystalline (LC) phases.

Department of Applied Chemistry, National Chi Nan University, Puli, Nantou, 545, Taiwan. E-mail: lilai@ncnu.edu.tw

† Electronic supplementary information (ESI) available: Experimental and supporting results. See DOI: https://doi.org/10.1039/d3ma00747b

Additionally, porous materials such as metal organic frameworks (MOFs), covalent organic frameworks (COFs) and H-bonded organic frameworks (HOFs) have attracted great attention in recent decades because the void spaces inside their frameworks are available for guest molecules.[34–40] Although HOFs are probably fabricated with 3-D dimensions, their frameworks are rather unstable in comparison to the fixed and stable frameworks of MOFs and COFs, and may collapse when the guest molecules are removed. Very recently, dendrimers with flexible frameworks were also observed to contain void spaces for external gases or volatile organic compounds (VOCs) in their solid state.[4,5,7,41] As HOFs, the void spaces of dendrimers were observed to expand or shrink under gases.[4] Therefore, dendritic LC materials that are constructed only by 1-D or 2-D interactions are very unlikely to maintain free void spaces, although several articles have reported the possibility of free pores in the mesogenic or solid state of LC materials.[42–44] However, porous LC materials are very useful because they possess well-ordered arrangements over a long range and thus exhibit good sensitivity for detecting gases, metal ions or volatile organic compounds, and therefore have valuable applications in related areas.

Previously, we first reported an LC dendrimer that self-assembled into columnar stacks and thus possessed free void space for directly adsorbing Xe in the mesogenic or solid state by introducing a non-coplanar unit, the amidopiperazine moiety, on its dendritic frame.[12] Here, using a different strategy for preparing porous LC materials, we further synthesize two CN-containing dendrons with different lengths of central corner, which couple into dendrimer-like molecules *via* dipole–dipole interaction, thus exhibiting a mesogenic phase upon thermal treatment. Because of the various lengths of central corner, the free void spaces fabricated by two dendrons are different, as determined on the basis of their BET isotherms. To the best of our knowledge, no mesogenic dendrons as solids have ever been reported to contain free pores in their dendritic framework so far, and we now wish to communicate the preliminary results.

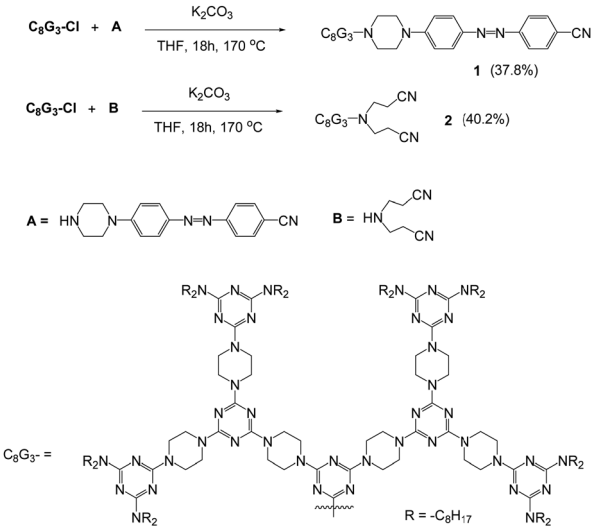

Scheme 1 Preparation of dendrons **1** and **2**.

Dendron **C_8G_3Cl** was prepared according to the literature[45] and was further treated with **A** or **B** in a sealed tube at 170 °C for 18 hours to give dendrons **1** or **2** in reasonable yields (Scheme 1). Dendrons **1** and **2** were both identified using NMR spectroscopy, mass spectrometry and microanalysis. The mass spectra of dendron **1** and **2** obtained by the MALDI-TOF technique show peaks at 3266.0 and 3097.9, respectively, from the corresponding $[M + H]^+$ ion (Fig. S1, ESI†). Compound **B** is commercially available, and the synthetic procedure for compound **A** is provided in the ESI.†

Dendrons **1** and **2** were observed to exhibit good stability upon thermal treatment, and both their decomposition temperatures (T_d, 5% weight loss) were found to be over 300 °C by thermogravimetric analysis (TGA). Particularly, dendron **1** is even stable up to ~420 °C (Fig. 1a). The TGA investigation of **1** under N_2 reveals that the weight percentage of **1** slightly increases about 1.94% before decomposition, which was not observed for dendron **2** (Fig. S2, ESI†). This phenomenon may be attributed to the trapping of nitrogen within the framework of **1**. This suggests that dendron **1** should have a free void space in the solid or mesogenic state, which is discussed later.

Both dendrons **1** and **2** show hexagonal columnar phases upon heating and cooling treatment. Their liquid crystalline (LC) properties are summarized in Table 1. Dendrons **1** and **2** with different central cores have similar dendritic structures. Upon heating, dendron **1** starts to exhibit a mesogenic phase at ~196 °C and becomes isotropic at ~201 °C; its mesogenic range upon heating (~4 °C) is much smaller than that of dendron **2** (~18 °C), as demonstrated in Table 1. In their cooling processes, a similar behaviour was also observed; the mesogenic ranges of **1** and **2** were observed to be ~44 and ~53 °C, respectively. This is probably because the **A** moiety of dendron **1** is rigid and the **B** moiety of dendron **2** is rather flexible.

The columnar phases of dendron **1** and **2** were also supported by observing the domain texture under a polarizing optical microscope (POM) and further confirmed *via* powder X-ray diffraction (Fig. 2). Sharp peaks at 33.76 and 32.77 Å were detected in the small-angle region for **1** and **2**, respectively, and are indexed as d_{10}. Two additional weak signals at 19.44 and 16.85 Å for **1**, as well as at 19.44 and 16.85 Å for **2**, are indexed as d_{11} and d_{20}, respectively. The XRD pattern is indicative of a hexagonal columnar phase for dendrons **1** and **2**, and the lattice constants a were calculated to be 39.09 and 37.94 Å, respectively. The broad hump signals at 12.78 and 13.03 Å observed in Fig. 2a and b, respectively, may arise from the reflection of the disk layer.

As mentioned earlier, dendron **1** shows a slight increase in weight percentage during the TGA investigation because of N_2 trapping, which indicates the existence of free void spaces within the dendritic framework **1**. Therefore, dendron **1** was studied using Brunauer–Emmett–Teller (BET) analysis. At 195 K (−78 °C), the adsorption capacity of dendron **1** for CO_2 is approximately 18.9 $cm^3\ g^{-1}$, and thus the BET surface area of **1** is calculated to 34.15 $m^2\ g^{-1}$ (Fig. 3). Dendron **2** behaved similarly at 195 K (−78 °C), with an adsorption capacity of 10.6 $cm^3\ g^{-1}$ and a BET surface area of 20.41 $m^2\ g^{-1}$ (Fig. S3, ESI†). This definitely confirms that dendrons **1** and **2** consist of free pores in the solid state for gas adsorption. Based on the BET study of dendron **1** at 273 K (0 °C), as shown in Fig. 3, its pore sizes were observed to have major distributions at 5.06, 6.11 and 7.51 Å, respectively (Fig. 4). As there was no significant absorption of CO_2 for dendron **2** at 273 K (0 °C), its pore distribution cannot be investigated accordingly.

It is interesting to note that dendrons **1** and **2** have the same linking and peripheral groups, with variation only in the corresponding core moiety. Apparently, the molecular length of compound **A** is longer than that of compound **B**. When two

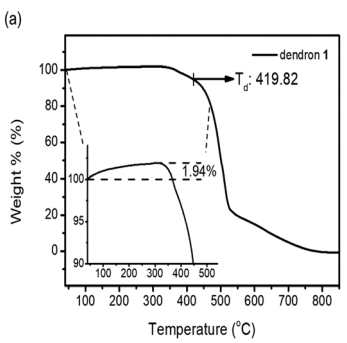

Fig. 1 TGA of dendron **1** from 40 to 850 °C at a heating rate of 10 °C min^{-1} under N_2.

Table 1 Phase transition temperatures of dendrons **1** and **2**. Their corresponding enthalpies are given in parentheses (J g^{-1})

Dendron 1	Cryst	196.8 (3.8) ⇌ 152.0 (−8.3)	Col_h	201.0 (1.8) ⇌ 196.6 (−4.2)	Iso
Dendron 2	Cryst	132.5 (34.9) ⇌ 92.6 (−31.0)	Col_h	150.1 (1.9) ⇌ 145.9 (−1.7)	Iso

Cryst., Col_h and Iso denote the crystalline, hexagonal columnar, and isotropic phases, respectively. The transition temperatures and corresponding enthalpies were recorded for the second cycles between the isotropic phases and room temperatures.

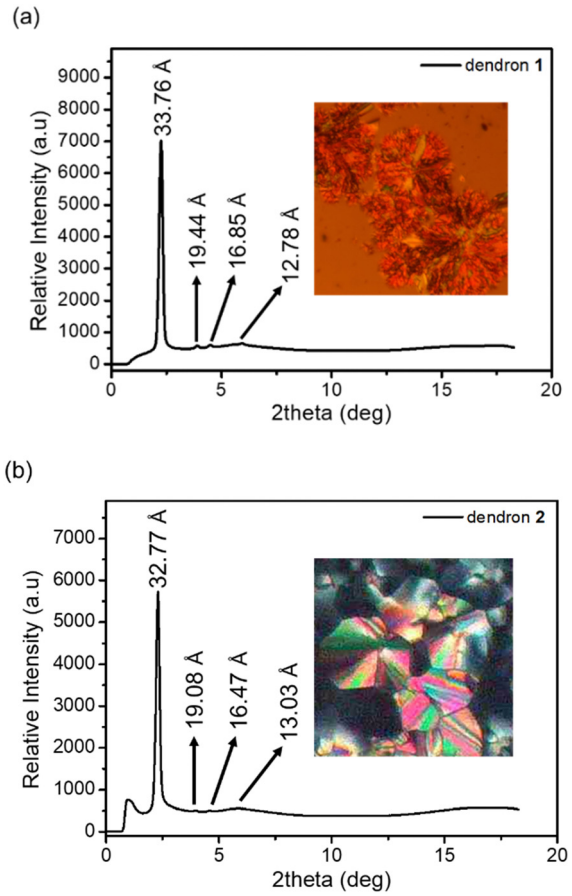

Fig. 2 (a) XRD data and POM image of dendron **1** at ~190 °C upon cooling. (b) XRD data and POM image of dendron **2** at ~140 °C upon cooling.

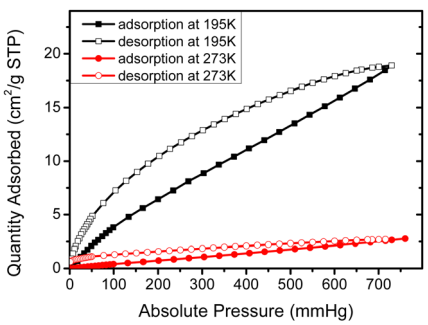

Fig. 3 BET isotherms of dendron **1** at 195 K and 273 K.

dendrons are located in a head-to-head arrangement due to the strong dipole–dipole interaction, the corresponding void spaces of dendrons **1** and **2** should be different from each other, as illustrated in Fig. 5. To further confirm the fabrication of the void spaces by the two dendritic molecules, calculation of the dipole moments of cores **A** and **B** were thus performed. The frequency and geometry optimizations of **A** were completed using Gaussian 09 at the B3LYP/6-31G** level first, and the dipole moment of moiety **A** was estimated to be 8.72 Debye. The dipole moment of moiety **B** was calculated to be 7.85 Debye,

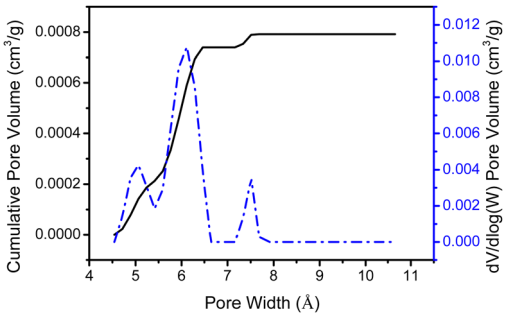

Fig. 4 Pore size distribution of dendron **1**.

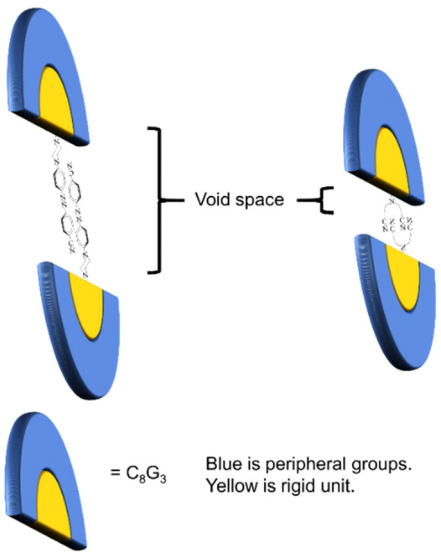

Fig. 5 A conceptual diagram of the stacking arrangement of dendrons **1** and **2** showing the different void spaces fabricated.

which is similar to that of moiety **A** (Fig. 6). This means that the strong dipole in the dendritic cores of both **1** and **2** is sufficient to cause the two dendritic molecules to self-assemble in a head-to-head arrangement and thus fabricate free void space in the solid state. The calculation details are provided in the ESI.†

As dendron **1** possesses a N=N functionality, *cis* and *trans* isomerization upon UV radiation or thermal treatment can be expected.[46] Dendron **1** was thus heated to its isotropic state rapidly and then gradually cooled to 194 °C at a rate of

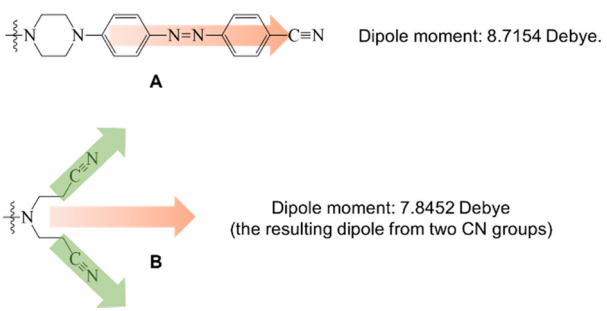

Fig. 6 Polarity direction and dipole moment of core **A** and **B**.

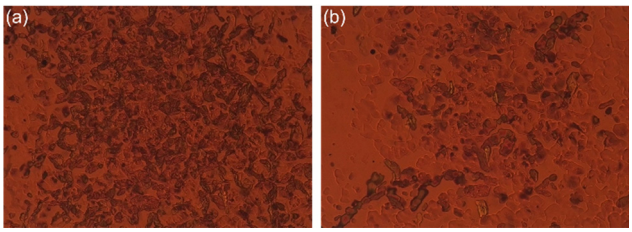

Fig. 7 (a) POM texture of dendron **1** at 194 °C; (b) POM texture of dendron **1** at 194 °C after irradiation for ~6 min.

2 °C min^{-1}. At this temperature, a mixed mesogenic and isotropic phase for dendron **1** was observed under POM, which was subsequently irradiated with UV light with a 365 nm wavelength for approximately six minutes (Fig. 7a). As a result, the isotropic/mesogenic ratio significantly increased, as shown in Fig. 7b, which is attributed to *cis–trans* isomerization of the N=N double bond under UV radiation. Because dendron **1** becomes a mixture with the *cis* and *trans* conformations after irradiation, the isotropic-to-Col_h phase transition temperature thus decreases, and a greater isotropic/mesogenic was thus observed under POM. Another possibility for this observation is that dendron **1** with the N=N *cis* conformation may not show the mesogenic phase at this temperature.

Conclusions

In summary, we have successfully prepared two dendrons with strong polar groups in the core moiety, and both dendrons were observed to exhibit mesogenic phases upon thermal treatment. Because of the dipole–dipole interaction, the two dendrons were arranged in a head-to-head arrangement, and thus, the corresponding free void spaces were fabricated by the dendrons. As the molecular length of the core moiety in each dendron is different, the free void space between dendrons in the head-to-head arrangement was also observed to be different, which was directly proved by the BET isotherms. As dendron **1** has an N=N functionality, at the temperature of the mixed phase of the mesogenic and isotropic state, isomerization between the *cis* and *trans* conformation was also observed under UV radiation, which may provide a switching mechanism for electronic design in possible applications.

Conflicts of interest

There are no conflicts to declare.

Acknowledgements

We thank the National Synchrotron Radiation Research Center for providing the powder XRD services. This research was funded by the National Chi Nan University and the Ministry of Science and Technology, Taiwan (111-2113-M-260-003).

Notes and references

1 G. R. Newkome, C. N. Moorefield, F. Vögtle and G. Chemist, *Dendrimers and dendrons: concepts, syntheses, applications*, Wiley Online Library, 2001.
2 A.-M. Caminade, C.-O. Turrin, R. Laurent, A. Ouali and B. Delavaux-Nicot, *Dendrimers: towards catalytic, material and biomedical uses*, John Wiley & Sons, 2011.
3 T. Kato, J. Uchida, T. Ichikawa and T. Sakamoto, *Angew. Chem., Int. Ed.*, 2018, **57**, 4355–4371.
4 C.-H. Lee, M.-R. Tsai, Y.-T. Chang, L.-L. Lai, K.-L. Lu and K.-L. Cheng, *Chem. – Eur. J.*, 2013, **19**, 10573–10579.
5 Y.-C. Lu, C.-Y. Chien, H.-F. Hsu and L.-L. Lai, *Molecules*, 2021, **26**, 4862.
6 Y.-H. Tang, M. Cangiotti, C.-L. Kao and M. F. Ottaviani, *J. Phys. Chem. B*, 2017, **121**, 10498–10507.
7 Z.-T. Gu, C.-H. Tzeng, H.-J. Chien, C.-C. Chen and L.-L. Lai, *Int. J. Mol. Sci.*, 2022, **23**, 11155.
8 L.-L. Lai, J.-W. Hsieh, K.-L. Cheng, S.-H. Liu, J.-J. Lee and H.-F. Hsu, *Chem. – Eur. J.*, 2014, **20**, 5160–5166.
9 M.-J. Tsai, J.-W. Hsieh, L.-L. Lai, K.-L. Cheng, S.-H. Liu, J.-J. Lee and H.-F. Hsu, *J. Org. Chem.*, 2016, **81**, 5007–5013.
10 C.-H. Lee, C.-C. Huang, C.-Y. Li, L.-L. Lai, J.-J. Lee and H.-F. Hsu, *J. Mater. Chem. C*, 2019, **7**, 14232–14238.
11 Y.-C. Lu, H.-F. Hsu and L.-L. Lai, *Nanomaterials*, 2021, **11**, 2112.
12 Y.-C. Lu, R. Anedda, H.-H. Chen, H.-C. Hsu, S.-J. Hsu, C. Ratcliffe, L.-L. Lai, J. Ripmeester and H.-F. Hsu, *J. Mater. Chem. C*, 2023, **11**, 3710–3714.
13 K. Albrecht, K. Matsuoka, K. Fujita and K. Yamamoto, *Mater. Chem. Front.*, 2018, **2**, 1097–1103.
14 C.-X. Liu, H. Wang, J.-Q. Du, K.-Q. Zhao, P. Hu, B.-Q. Wang, H. Monobe, B. Heinrich and B. Donnio, *J. Mater. Chem. C*, 2018, **6**, 4471–4478.
15 P. Pieper, V. Russo, B. Heinrich, B. Donnio and R. Deschenaux, *J. Org. Chem.*, 2018, **83**, 3208–3219.
16 V. Iguarbe, J. Barberá and J. L. Serrano, *Liq. Cryst.*, 2020, **47**, 301–308.
17 A. Concellón, T. Liang, A. P. H. J. Schenning, J. L. Serrano, P. Romero and M. Marcos, *J. Mater. Chem. C*, 2018, **6**, 1000–1007.
18 B. M. Rosen, C. J. Wilson, D. A. Wilson, M. Peterca, M. R. Imam and V. Percec, *Chem. Rev.*, 2009, **109**, 6275–6540.
19 H.-J. Sun, S. Zhang and V. Percec, *Chem. Soc. Rev.*, 2015, **44**, 3900–3923.
20 V. Percec and Q. Xiao, *Isr. J. Chem.*, 2021, **61**, 530–556.
21 V. Percec and Q. Xiao, *Bull. Chem. Soc. Jpn.*, 2021, **94**, 900–928.
22 V. Percec, C. H. Ahn, G. Ungar, D. J. P. Yeardley, M. Möller and S. S. Sheiko, *Nature*, 1998, **391**, 161–164.
23 V. Percec, M. Glodde, T. K. Bera, Y. Miura, I. Shiyanovskaya, K. D. Singer, V. S. K. Balagurusamy, P. A. Heiney, I. Schnell, A. Rapp, H. W. Spiess, S. D. Hudson and H. Duan, *Nature*, 2002, **419**, 384–387.
24 G. Ungar, Y. Liu, X. Zeng, V. Percec and W.-D. Cho, *Science*, 2003, **299**, 1208–1211.

25 S. D. Hudson, H. T. Jung, V. Percec, W. D. Cho, G. Johansson, G. Ungar and V. S. K. Balagurusamy, *Science*, 1997, **278**, 449–452.
26 X. Zeng, G. Ungar, Y. Liu, V. Percec, A. E. Dulcey and J. K. Hobbs, *Nature*, 2004, **428**, 157–160.
27 V. Percec, A. E. Dulcey, V. S. K. Balagurusamy, Y. Miura, J. Smidrkal, M. Peterca, S. Nummelin, U. Edlund, S. D. Hudson, P. A. Heiney, H. Duan, S. N. Magonov and S. A. Vinogradov, *Nature*, 2004, **430**, 764–768.
28 V. Percec, P. Chu, G. Ungar and J. Zhou, *J. Am. Chem. Soc.*, 1995, **117**, 11441–11454.
29 M. Marcos, R. Martín-Rapún, A. Omenat and J. L. Serrano, *Chem. Soc. Rev.*, 2007, **36**, 1889–1901.
30 L.-L. Lai, C.-H. Lee, L.-Y. Wang, K.-L. Cheng and H.-F. Hsu, *J. Org. Chem.*, 2008, **73**, 485–490.
31 W.-T. Chuang, T.-Y. Lo, Y.-C. Huang, C.-J. Su, U. S. Jeng, H.-S. Sheu and R.-M. Ho, *Macromolecules*, 2014, **47**, 6047–6054.
32 G.-C. Kuang, X.-R. Jia, M.-J. Teng, E.-Q. Chen, W.-S. Li and Y. Ji, *Chem. Mater.*, 2012, **24**, 71–80.
33 M. Park, D.-G. Kang, Y.-J. Choi, W.-J. Yoon, J. Koo, S.-H. Park, S. Ahn and K.-U. Jeong, *Chem. – Eur. J.*, 2018, **24**, 9015–9021.
34 Y.-F. Han, Y.-X. Yuan and H.-B. Wang, *Molecules*, 2017, **22**, 266.
35 Y.-C. Lu, C.-H. Lee, H.-H. Kuo, H.-C. Chiang, C.-T. Yao, H.-L. Sung, G.-H. Lee and L.-L. Lai, *Cryst. Growth Des.*, 2020, **20**, 6421–6429.
36 A. Moya, M. Hernando-Pérez, M. Pérez-Illana, C. San Martín, J. Gómez-Herrero, J. Alemán, R. Mas-Ballesté and P. J. de Pablo, *Nanoscale*, 2020, **12**, 1128–1137.
37 K. Geng, V. Arumugam, H. Xu, Y. Gao and D. Jiang, *Prog. Polym. Sci.*, 2020, **108**, 101288.
38 Z.-Z. Gao, Z.-K. Wang, L. Wei, G. Yin, J. Tian, C.-Z. Liu, H. Wang, D.-W. Zhang, Y.-B. Zhang, X. Li, Y. Liu and Z.-T. Li, *ACS Appl. Mater. Interfaces*, 2020, **12**, 1404–1411.
39 M. Firoozi, Z. Rafiee and K. Dashtian, *ACS Omega*, 2020, **5**, 9420–9428.
40 S. Mallakpour, E. Azadi and C. M. Hussain, *New J. Chem.*, 2021, **45**, 13247–13257.
41 C.-H. Lee, D. V. Soldatov, C.-H. Tzeng, L.-L. Lai and K.-L. Lu, *Sci. Rep.*, 2017, **7**, 3649.
42 K. Banlusan, E. Antillon and A. Strachan, *J. Phys. Chem. C*, 2015, **119**, 25845–25852.
43 M. Lehmann, M. Dechant, M. Lambov and T. Ghosh, *Acc. Chem. Res.*, 2019, **52**, 1653–1664.
44 M. Lehmann, M. Dechant, M. Holzapfel, A. Schmiedel and C. Lambert, *Angew. Chem., Int. Ed.*, 2019, **58**, 3610–3615.
45 Y.-C. Lu, Y.-T. Hsu, T.-Y. Yang, I. C. Liou, S.-W. Wang, P.-C. Huang, J.-J. Lee, L.-L. Lai and H.-F. Hsu, *Nanomaterials*, 2022, **12**, 185.
46 E. Merino and M. Ribagorda, *Beilstein J. Org. Chem.*, 2012, **8**, 1071–1090.